Kathmandu University Journal of Science, Engineering and Technology, Vol. 19, No. 2, June 2025

Kathmandu University
Journal of Science, Engineering and Technology

Assessing flood susceptibility and frequency analysis in himalayan river basins: A GIS-based multi-criteria approach

Binisha Shrestha *[a b], Eva Rajbhandari[a], Rijan Bhakta Kayastha[a], Sujan Shrestha[c], and Dewasis Dahal[c]

[a]Department of Environmental Science and Engineering, School of Science, Kathmandu University, Dhulikhel, Nepal.
[b]Department of Geosciences, Texas Tech University, Lubbock, Texas, USA.
[c]School of Civil, Environmental, and Infrastructure Engineering, Southern Illinois University, Carbondale, Illinois, USA.

Abstract

Flooding is a recurrent issue in Nepal during the monsoon season. This study assesses flood susceptibility zones in Himalayan River basins, specifically Tamakoshi and Indrawati River Basin, Nepal utilizing Geographic Information Systems (GIS) and multi-criteria analysis. Additionally, it employs Gumbel's distribution method for flood frequency analysis, estimating potential flood discharges for different return periods (2, 5, 10, 50, and 100 years). The critical flood causative factors like slope, elevation, land use/land cover, rainfall intensity, and river proximity are analyzed in this study using weighted multi-criteria overlay methods to produce flood-prone areas. Because the study areas are part of mountainous catchment areas, these regions have steep slopes, meaning surface runoff velocity is increased, ground infiltration of water decreases, and flood risks increase. GIS-based weighted overlay analysis identified approximately 26.6% of the Indrawati Basin and 25.4% of the Tamakoshi Basin as highly flood susceptible zones. The predicted flood discharges for a 100-year return period are 1566.59 m^3/s for Indrawati River Basin and 1821.87 m^3/s for Tamakoshi River Basin. The findings will support regional flood hazard management strategies and contribute to disaster risk reduction efforts in Nepal.

Keywords: Flood; Flood susceptible zone; Weighted overlay; GIS; Return period.

1. Introduction

Flooding is a high-water stage natural disaster in which water overflows its natural or constructed banks and inundates normally dry terrain, such as a river inundating its floodplain [1]. Floods can be detrimental to communities, lasting days, weeks, or sometimes even longer [2]. Yearly, on average, an economic value of US$ 662 billion has been damaged from 1995 to 2015 due to floods [3]. Factors like climate change and its variability, intense precipitation, rapid increase in population, economic development, haphazard urbanization, deforestation, and land use have increased the vulnerability to more significant flood events [4]. In the global context, Asia remains the most flood-prone continent, with countries such as Nepal, India, Bangladesh, and China experiencing recurring flood disasters [5]. In Nepal, floods rank among the top three deadliest natural disasters, with monsoon-induced floods frequently destroying settlements, infrastructure, and livelihoods [6]. Nepal is a country with varying topography starting at the relatively flat and low (80 m) Ganges Plain in the south and steeply increasing to thousands of meters of elevation in the Himalayas [7]. During the monsoon season, massive rainfall, as much as 550 mm in 24 hours can send large flood pulses downstream through the steep and mountainous terrain resulting in flash floods and landslides in the hilly regions of Nepal [8]. When the flood reaches the plain, known as Terai, inundation of riverbanks causes recurrent and severe flooding in Nepal, as well as in neighboring country India [9]. Among the South Asian countries, Nepal is the second highest country which is under the risk of floods [10]. In between 1954 and 2018, Nepal experienced significant flood-related impacts, including around 7,599 fatalities and economic losses amounting to approximately USD 10.6 billion, with the period from 1971 to 2011 alone accounting for around 3,329 deaths, 3.9 million affected individuals, and USD 5.8 billion in damages; notably, the 2008 collapse of the Koshi Barrage's eastern embankments displaced about 3 million people in Bihar, India, exemplifying the severe and recurrent nature of flooding, which has resulted in an average annual death toll of approximately 300 people [11].

The Indrawati and Tamakoshi River Basins, both sub-basins of the Koshi River, experience severe flooding during the monsoon season [12]. The Tamakoshi River originates in Tibet and flows through Nepal's Dolakha and Ramechhap districts before merging with the Sapta Koshi River [13]. This river system is highly susceptible to flash floods, significantly when landslides near the Nepal-China border obstruct river flow, forming temporary dammed lakes [14]. The sudden collapse of these obstructions releases massive flood waves, causing catastrophic damage downstream [15]. Similarly, the Indrawati River, a tributary of the Sun Koshi River, experiences heavy monsoon rainfall that leads to severe flooding, particularly in the Melamchi-Indrawati watershed [16]. Settlements, markets, roads, bridges, and agricultural fields in the downstream areas suffer extensive yearly damage [17].

Additionally, the presence of multiple glacial lakes in the upper catchments of these river basins heightens the risk of Glacier Lake Outburst Floods (GLOFs), which can trigger sudden, high-magnitude flood events [18, 19]. Despite regular flooding, there haven't been many studies related to the assessment of flood risk in the study area. The lack of detailed flood risk maps and pre-

*Corresponding author. Email: binisshr@ttu.edu

dictive models makes it challenging for policymakers and disaster management authorities to implement effective flood mitigation and response strategies [20]. Several studies have been conducted globally and in Nepal to assess flood hazards using GIS and the Multi-Criteria Weighted Overlay Analysis method [21]. Previous research has focused on flood risk assessment at broader regional scales [22]. However, few studies have provided high-resolution flood susceptibility mapping for specific river basins such as Indrawati and Tamakoshi. While past studies have utilized Digital Elevation Models (DEMs) and hydrological modeling, they often lack localized calibration with observed flood events, limiting their accuracy in identifying high-risk flood zones [23]. Additionally, flood frequency analysis using probabilistic models such as Gumbel's distribution remains underutilized in Nepal's flood susceptibility research despite its effectiveness in estimating extreme flood events [24].

To bridge this gap, this paper conducts a comprehensive flood susceptibility assessment for the Indrawati and Tamakoshi River Basins using GIS and multi-criteria weighted overlay techniques. The paper integrates spatial and hydro-meteorological data to analyze flood-prone areas based on key topographical, climatic, and hydrological parameters. Additionally, the Gumbel distribution method, ideal for predicting extreme hydrological events, was employed for flood frequency analysis, estimating potential flood discharges for different return periods (2, 5, 10, 50, and 100 years). This paper aims to offer valuable insights for policymakers, urban planners, and disaster response teams by providing high-resolution flood hazard maps and predictive flood return period. The findings will contribute to improved flood preparedness, enhanced early warning systems, and sustainable land-use planning, ultimately reducing the socio-economic impacts of floods in the Indrawati and Tamakoshi River Basins.

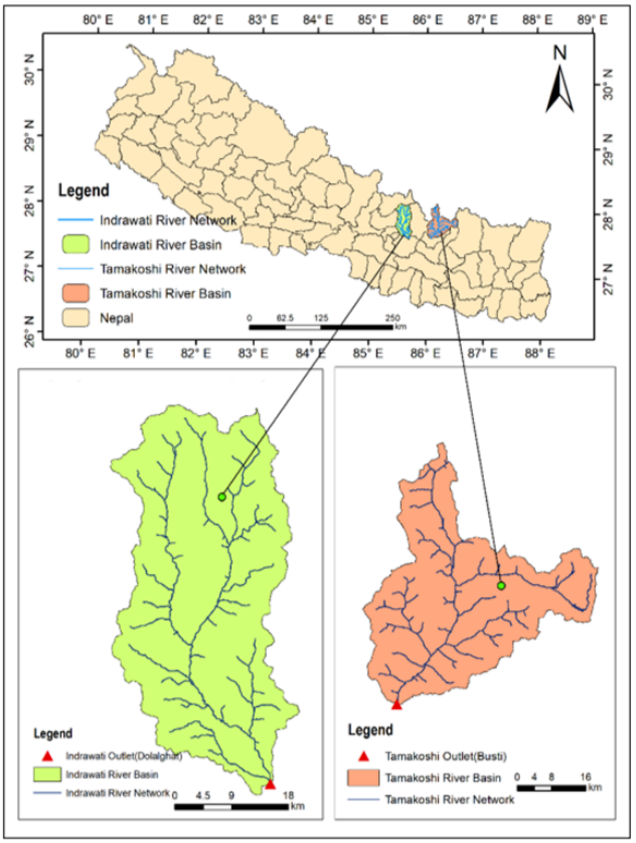

Figure 1: Location of study area a) Map of Nepal with Indrawati and Tamakoshi River Basin b) Map of Indrawati River Basin showing its outlet at Dolalghat c) Map of tamakoshi River Basin showing its outlet at Busti.

2. Materials and methods

2.1. Study area

The Indrawati and Tamakoshi River Basins, two significant tributaries of the Saptakoshi River in Nepal, make up the study area. The Indrawati River Basin, which spans from 27°37'11" N to 28°10'12" N latitude and 85°45'21" E to 85°26'36" E longitude, has a total catchment area of 1,228 km² and encompasses roughly 43% of Sindhupalchowk district and 11% of Kavrepalanchowk district in Bagmati Province. The river rises in the snow-capped Himalayan range and travels south until joining the Sunkoshi River at Dolalghat in the district of Kavrepalanchowk. Comparably, the Tamakoshi River Basin, which spans a catchment area of 1,489 km² and is situated in the Dolakha region of Bagmati Province, stretches from 27°37'42" N to 28°19'23" N latitude and 86°0'9" E to 86°34'24" E longitude. The Tamakoshi River rises in the Tibetan Himalayas and travels south before joining the Sunkoshi River. Rainfall in the Indrawati Basin ranges from 1,200 to 3,000 mm annually, with the monsoon season accounting for 80% of this total. The temperature fluctuates between 4°C and 33°C, while the relative humidity ranges from 60% to 90%. Likewise, Jiri station temperature records show summer highs of 25°C and winter lows of -2°C in the Tamakoshi Basin. With significant tributaries such as Melamchi, Yangri, Larke, Mahadev, Chaa, Handi, and Jhyangri, the Indrawati River has a hydrological length of 59 km and an average annual discharge of 75.06 m^3/s. With important tributaries like Lapche, Rongchar, and Rolwaling, the 92-kilometer Tamakoshi River has an average annual discharge of 66 m^3/s. Regarding geology, the Indrawati Basin comprises rough hills and mountains, with lower-altitude regions that are either cultivated or populated and steep high-altitude regions that are vulnerable to deep gullies [25]. In contrast, the exhumed mid-crustal core of the Himalayas, composed of phyllitic schist, paragneiss, and orthogneiss formations, dominates the Tamakoshi Basin [26]. Both basins are highly vulnerable to severe flood events due to their different geological, hydrological, and climatic circumstances, underscoring the need for thorough flood susceptibility assessment and mapping.

Table 1: Illustration of spatial data used and their sources.

S.N.	Data	Year	Resolution	Source
1.	ALOS PALSAR DEM	2021	12.5m	ASF
2.	Land Use/ Land Cover Map	2020	10m	ESri

2.2. Data used

The required spatial and hydrometeorological datasets are collected and used from different sources. Table 1 provides the data types used in this paper and their sources. DEM is used for topographic analysis, including slope and elevation mapping. The LULC map, from which the relevant tile covering both river basins is downloaded, classified, processed, and analyzed. According to the Esri Living Atlas, the LULC map is 98% accurate. A GIS environment is used to preprocess and analyze these data to produce themed maps depicting various flood conditioning factors.

Likewise, the nearest stations' hydrological (discharge) and meteorological (rainfall and temperature) data are collected from the Department of Hydrology and Meteorology, (DHM) Babarmahal, Kathmandu, Nepal. Table 2 represents the details of hydrometeorological stations used in this study.

Table 2: Hydro-Meteorological stations in our study area.

River Basin	Data Type	No. of Stations	Station Names	Duration	Frequency
Indrawati River Basin	Rainfall	6	Duwachaur, Nawalpur, Sarmathang, Baunepati, Mandan, Dhap	2000-2020	Monthly
	Discharge	1	Dolalghat	1995-2015	Daily
Tamakoshi River Basin	Rainfall	3	Jiri, Nagdaha, Charikot	2000-2020	Monthly
	Discharge	1	Busti	1995-2009	Daily

2.3. Data processing

The approach integrates spatial, hydrological, and meteorological data to develop flood susceptibility maps and conduct flood frequency analysis. The primary steps include watershed delineation, land use and land cover (LULC) classification, rainfall trend analysis, flood susceptibility weightage mapping, flood susceptibility zoning, and flood frequency analysis using Gumbel's method [27].

Watershed delineation is the first step of the study. It uses ALOS PALSAR DEM of 12.5m spatial resolution in ArcGIS 10.8.1. The spatial analyst tools in the Arc Toolbox allow hydrological calculations, including flow direction and accumulation, to generate stream networks. Negative values in the DEM are corrected using the fill algorithm from the Hydrology group of the Arc Toolbox. The pour point feature is used to select the outlet points of the river, with Dolalghat (Indrawati River) and Busti (Tamakoshi River) chosen as the main outlets shown in Table 2. Using this data, the watershed is delineated to obtain the basin area, which is then clipped and projected to the UTM Zone 45N coordinate system with the WGS_1984 datum. Similarly, the downloaded Land Use Land Cover (LULC) map is trimmed to extract the study area and classified into eight major categories: water bodies, snow/ice, vegetation land, settlements, bare lands, grasslands, shrublands, and forests. Land use is defined as the observable bio-physical cover of the watershed, while land cover is defined as the degree of human activities directly tied to land and making use of its resources [28].

Rainfall is a vital parameter that has been widely used in flood hazards and susceptibility mapping [29]. Floods are caused by a variety of factors, including heavy and strong rainfall [30]. Monthly mean precipitation data are obtained from the Department of Hydrology and Meteorology (DHM) which are used to analyze the climatic trends over the period of 2000-2020 for rainfall trend analysis. The 20-year period for rainfall trend analysis are selected as the duration of the study to ensure standardization among stations and an adequate record length. Rainfall data from six stations and three stations in case of Indrawati River Basin and Tamakoshi River Basin are collected from DHM respectively. The considered stations are mentioned in Table 3. The objective of selecting the network of stations is to cover all the climatic zones of both the river basin as far as possible. Thus, even if the two stations come from the same basin, there is a high probability that data obtained from these stations will vary from one another. However, due to the complex topography of the country and the limited number of stations available, this condition could not be satisfied, nevertheless, attention has been given so as to have as much spatial coverage as possible. As a result, stations with a short data period or with large inconsistency/missing data are discarded in order to ensure the quality and completeness of the available precipitation. The statistical analysis of linear regression is used for identifying the trend in climatic variation based on the available precipitation and temperature data using Microsoft Excel and the obtained graph is plotted to see the trend.

2.3.1. Preparation of flood susceptibility weightage map

Flood susceptibility mapping for this study is conducted using ArcGIS 10.8.1 by incorporating five key factors: land use/land cover (LULC), slope, elevation, rainfall intensity, and proximity to the river [31]. The Multi-Criteria Evaluation (MCE) method, specifically the weighted overlay analysis, is applied to integrate these factors . Each thematic layer is developed using satellite-derived datasets and official records, then rasterized and categorized into five susceptibility classes: very high, high, moderate, low, and very low [32].

LULC data are extracted from the Esri 2020 global land cover map and reclassified based on the susceptibility level associated with each land type. Slope and elevation maps are generated from ALOS-PALSAR DEM using surface analysis tools in ArcGIS. Rainfall intensity is calculated using 2000–2020 monthly averages from DHM meteorological stations and interpolated through the Inverse Distance Weighted (IDW) method [33]. Stream networks are delineated from the DEM using flow accumulation tools, and multi-ring buffers at 500, 1000, and 1500-meter intervals are used to define river proximity zones [34]. These layers are then combined using the weighted overlay method to produce the final flood susceptibility map for both river basins [35].

The method used for composing the flood susceptibility weightage map is shown in Fig. 2(a). The factors that cause floods are determined in the first step, and the mutual interaction ratios are calculated. All the factors mentioned above, like slope, elevation, land use, land cover, rainfall intensity, and distance away from the river network, are the interacting factors.

As shown in Fig. 2(b), a straight line between two factors indicates that it primarily affects the other. The dotted line between the two factors indicates that it has a secondary effect on others. For example, while distance from the river network primarily affects land use, it also has a secondary effect on the slope. Likewise, rainfall intensity primarily affects the distance away from the river network and has a secondary effect on land use. In order to measure two different effects, one (1) point is assigned to the significant factor, and half (0.5) point is assigned to the minor factor. Equal weighting was chosen based on Saaty's Analytical Hierarchy Process (1980), consultations with local hydrologists, and expert judgment.

Geological differences were critically evaluated by examining the lithological, structural, and geomorphological settings of both river basins. The Indrawati basin primarily consists of fragile sedimentary formations and rugged topography, while the Tamakoshi basin is underlain by high-grade metamorphic rocks, such as schists and gneisses. These geological features potentially influence erosion rates and slope stability. However, in the context of flood susceptibility, driven mainly by surface runoff, land use changes, slope gradients, rainfall intensity, and proximity to rivers, the geological substrate exerts only a secondary influence. Field consultations and expert inputs concluded that while geology might affect localized landslides or sediment load, its effect on the overall flood susceptibility zoning was minimal compared to topographic and hydrometeorological factors [36]. Therefore,

Table 3: Average yearly precipitation data for different stations with their respective XY coordinates.

S.N.	Station name & Index No.	Latitude (x)	Longitude(Y)	Elevation	Average yearly rainfall(mm)
a	For Indrawati River basin				
1	Nawalpur (1008)	27°48’	85°37’	1592	2278.62
2	Sarmathang (1016)	27°57’	85°36’	2625	3321.91
3	Duwachaur (1017)	27°52’	85°34’	1550	1968.65
4	Baunepati (1018)	27°47’	85°34’	845	1396.065
5	Mandan (1020)	27°42’	85°39’	1365	908.07
6	Dhap (1025)	27°55’	85°38’	1240	3030.8
b	For Tamakoshi River basin				
1	Nagdaha (1101)	27°41’	86°06’	850	2215.59
2	Charikot (1102)	27°40’	86°03’	1940	1285.65
3	Jiri (1103)	27°38’	86°14’	2003	2499.25

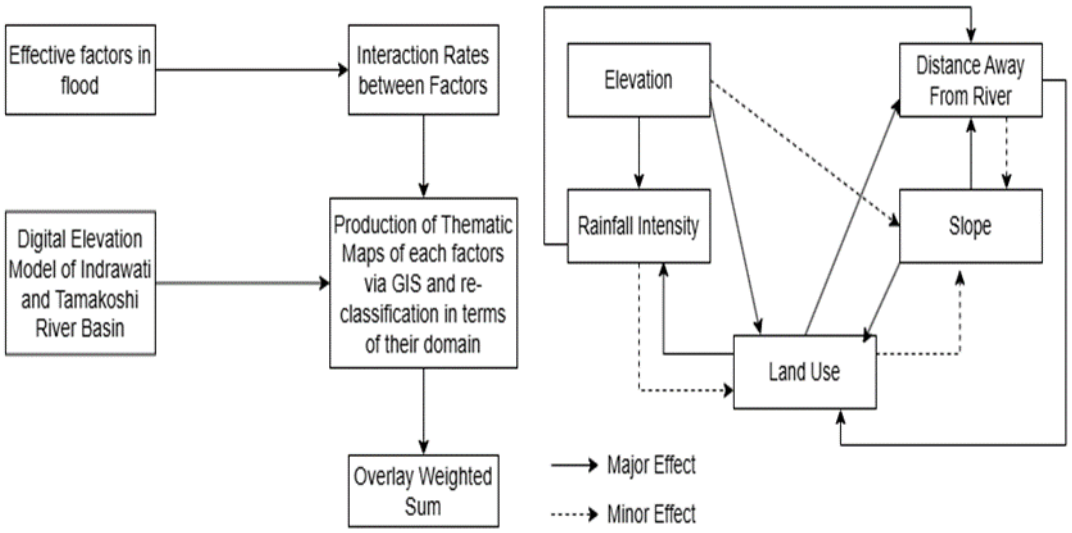

Figure 2: (a) Methods for composing the flood hazard weightage map of different factors (b) Methods to determine the major and minor effects between the factors.

assigning equal weights to both basins is deemed reasonable and scientifically valid, especially since the susceptibility maps are derived from surface characteristics rather than subsurface geology [37].

In the next phase, a factor rate is calculated as the sum of the impacts on others. The weighing approach has been applied by giving different impacts on flood hazards. The ratio determined for the factors is shown in Table 4. Land use is the descriptive factor within these factors, and others have the numerical values. The basic rule to estimate flood susceptible areas is a classification based on the field's degree of disaster risk. The effect of each factor is mapped in the form of five different susceptibility levels: very high, high, moderate, low, and very low. This approach involves multiplying the calculated ratio and its determined weight to calculate the total weight for each factor [38]. The thematic labeled map is combined with the approach of the weightage overlay method, and the final flood susceptibility zone map showing risk areas is produced [39, 40].

2.3.2. Flood frequency analysis

Flood frequency analysis employs probability models, like Gumbel's Extreme Value Distribution, to predict peak discharges based on historical flood records. Gumbel's method, widely used for its suitability in cases of limited, homogeneous, and independent flow data from less regulated rivers, effectively predicts extreme flood events. In this study, annual peak discharge data from 2000–2015 for the Indrawati and Tamakoshi Rivers is analyzed using Gumbel's distribution to estimate flood discharges for return periods of 2, 5, 10, 50, and 100 years.

2.3.3. Flood susceptibility analysis

Flood Susceptibility Analysis is computed by weighted sum overlay of the slope, elevation, land use, land cover, rainfall intensity, and distance away from river network developed factors. The weights for each factor are given through discussion with concerned bodies and based on literature. The relevant maps for this investigation are prepared using ArcGIS 10.8.1. For our study, we employed the Multi-Criteria Evaluation Method's weighted overlay analysis approach, in which each criterion is given a weight based on its relevance. Following the mapping, each element is assigned a rating based on its anticipated importance in triggering floods. Weighted Overlay Analysis is used to integrate the data layers into the GIS environment and create the susceptible zone map that resulted. The area covered by the created map is further divided into five hazard zones: very high, high, moderate, low, and very low. The overall framework for the study is shown in Fig. 3.

3. Results and discussions

3.1. Rainfall distribution analysis

The monthly mean time series monthly precipitation for the period of 2000-2020 are analyzed and processed to calculate the annual average rainfall by using the parametric linear regression method. The network of stations is chosen to encompass all the climatic zones of each river as far as possible.

In case of the Indrawati River Basin, the study reveals that over the period of 2000 to 2020 A.D. year, the average annual precipitation has significantly increased in major three meteorological stations. It has increased by 30.981 mm per year, 45.467 mm per year and 12.17 mm per in Sarmathang, Baunepati and Dhap rainfall stations respectively. However, it has decreased by 54.94 mm per year, 10.426 mm per year and 16.922 mm per year in Duwachaur, Mandan and Nawalpur rainfall station respectively. So, analysing the rainfall trend in Indrawati River Basin, both increasing/upward trend and decreasing/downward trend can be seen. Looking at the trend, we can know that there is high precipitation in areas like Sarmathang, Baunepati and Dhap whereas there is low precipitation in the areas like Duwachaur, Nawalpur and Mandan. The increased precipitation results in flooding, whereas the decreased precipitation results in drought. The rainfall trend of Indrawati River Basin is shown in Fig. 4.

Similarly, in case of Tamakoshi River Basin, the study reveals that over the same period of time 2000 to 2020, the average annual precipitation has significantly decreased in two rainfall station whereas it has increased by few mm per year in one rainfall station. The rainfall has increased by 4.0335 mm per year in Jiri whereas it has decreased by 37.49 mm per year in Nagdaha and 11.37 mm per year in Charikot. Overall, the graph in Fig. 5 indicates the decreasing trend of rainfall in Tamakoshi River Basin.

3.2. Flood susceptibility assessment

After delineating the watershed, the catchment area of the Indrawati River Basin and Tamakoshi River Basin are found to be 1228 sq.km. and 1489 sq. km. respectively. Flood risk is greatly influenced by slopes, with flatter terrains being more vulnerable to flooding because of slower drainage. Slopes between 0° and 20° were classified as very high hazard in the Indrawati River Basin, accounting for 21.27% of the total flood risk, while slopes over 80° were considered minimally susceptible. Similarly, 22.5% of the Tamakoshi River Basin's slopes, which range from 0° to 16°, were categorized as highly susceptible. In all basins, higher slope gradients demonstrated reduced susceptibility because of faster water circulation, which lessens the likelihood of water storage. Elevation also influences flood susceptibility, with low-lying areas being more vulnerable. Areas between 572-1404 meters were categorized as having very high susceptible in Indrawati, which accounted for 26.6% of the risk of flooding. Similarly, higher elevations above 4194 meters in Indrawati and 5671 meters in Tamakoshi were the least affected by flooding, whereas elevations between 823 and 2035 meters in Tamakoshi posed the most significant risk at 25.4%.

Land use and land cover influence flood susceptibility by affecting runoff and infiltration rates. The most significant risk of flooding was found in water bodies, ice/snow, and bare areas, which accounted for 26.6% of the overall danger in Indrawati and 24% in Tamakoshi. Shrublands and settlements comprised 20% and 18% of the basins, respectively, and were categorized as high-hazard zones. Vegetation and grasslands demonstrated moderate susceptibility, with weights of 15% in Indrawati and 16% in Tamakoshi. Forested areas had the lowest risk due to their ability to absorb excess water, covering 10-12% of the flood-prone zones. Flood risks are directly impacted by rainfall intensity, as higher precipitation causes more runoff. The Indrawati River Basin showed that areas receiving 2839-3321 mm of annual rainfall were at the highest flood risk, covering 15.95% of the region. Similar trends appeared in Tamakoshi, where the most significant risk of flooding was caused by rainfall between 2255 - 2498 mm, which accounted for 14.8% of the total. Areas with lower rainfall, such as those in Indrawati (1391-1873 mm) and Tamakoshi (1528-1770 mm), are identified as low-susceptible zones, accounting for approximately 6–7% of the area.

Proximity to rivers significantly influences flood susceptibility, with areas within 500 meters of riverbanks facing the highest susceptibility levels. In both basins, regions in this range contributed 9.58% (Indrawati) and 8.9% (Tamakoshi) to total flood risk. Locations between 500-1000 meters showed moderate flood risks, whereas areas beyond 1000 meters had minimal exposure, comprising around 2.5-3% of the total classification. Table 6 and Fig. 6 show the overall weightage scenario and related susceptibility ranges of each factor that causes flood in these two river basins.

Table 4: Major effect and minor effect of different interacting factors.

S.N.	Factors	Interaction between factors	Rates (b)
1.	Slope	2 (major) + 0 (minor)	$(2 * 1) + (0 * 0.5) = 2$
2.	Elevation	2 (major) + 1 (minor)	$(2 * 1) + (1 * 0.5) = 2.5$
3.	Land use land cover	2 (major) + 1 (minor)	$(2 * 1) + (1 * 0.5) = 2.5$
4.	Rainfall intensity	1 (major) + 1 (minor)	$(1 * 1) + (1 * 0.5) = 1.5$
5.	Distance away from river network	1 (major) + 1 (minor)	$(1 * 1) + (1 * 0.5) = 1.5$

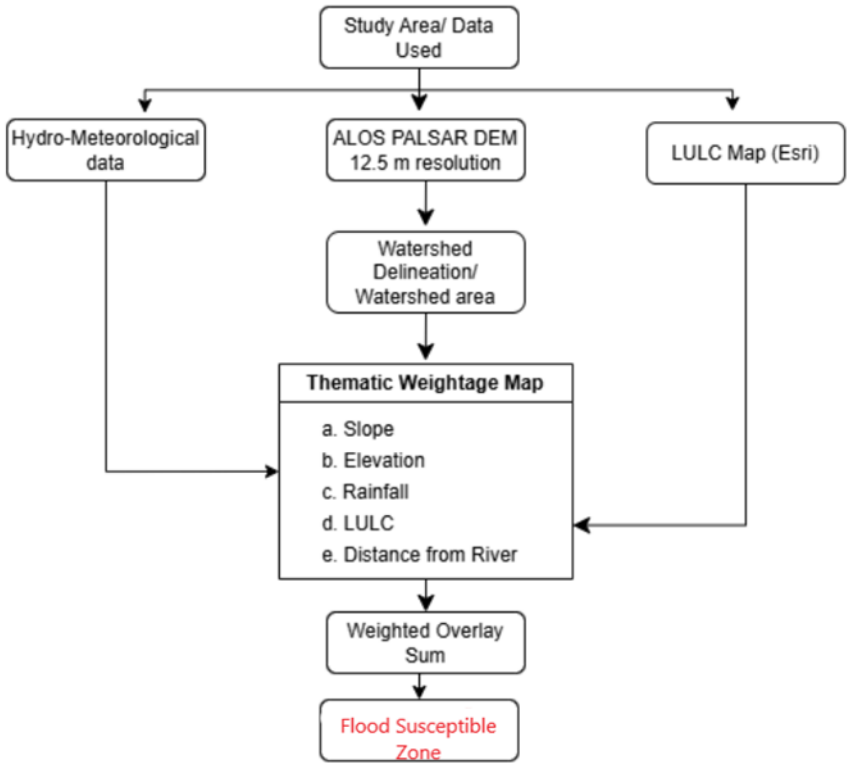

Figure 3: Methodology flowchart for flood susceptibility assessment using integrated GIS and MCE's weighted overlay sum method.

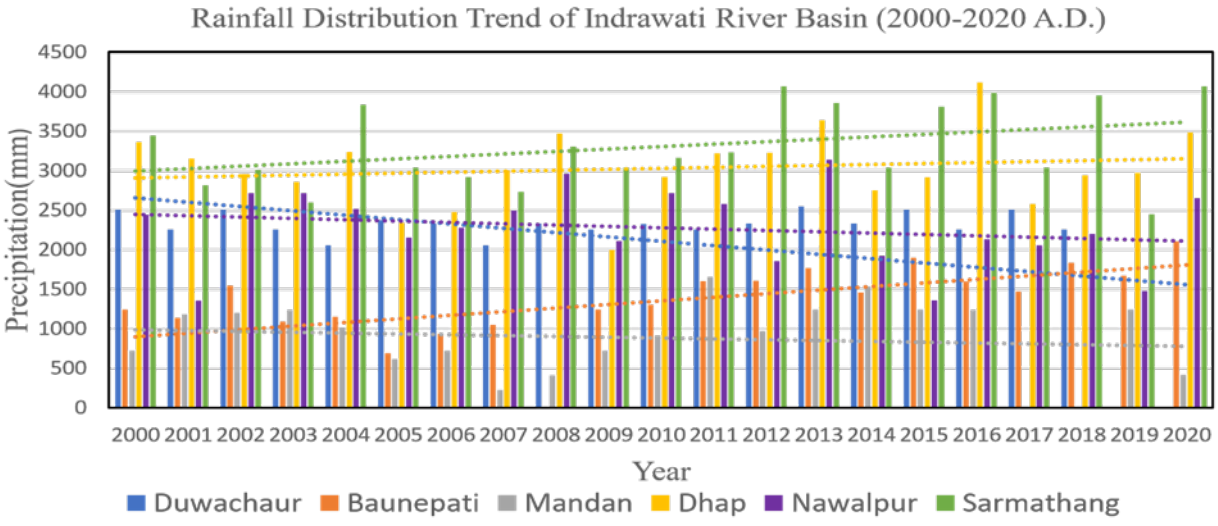

Figure 4: Rainfall distribution trend of Indrawati River Basin from 2000 to 2020.

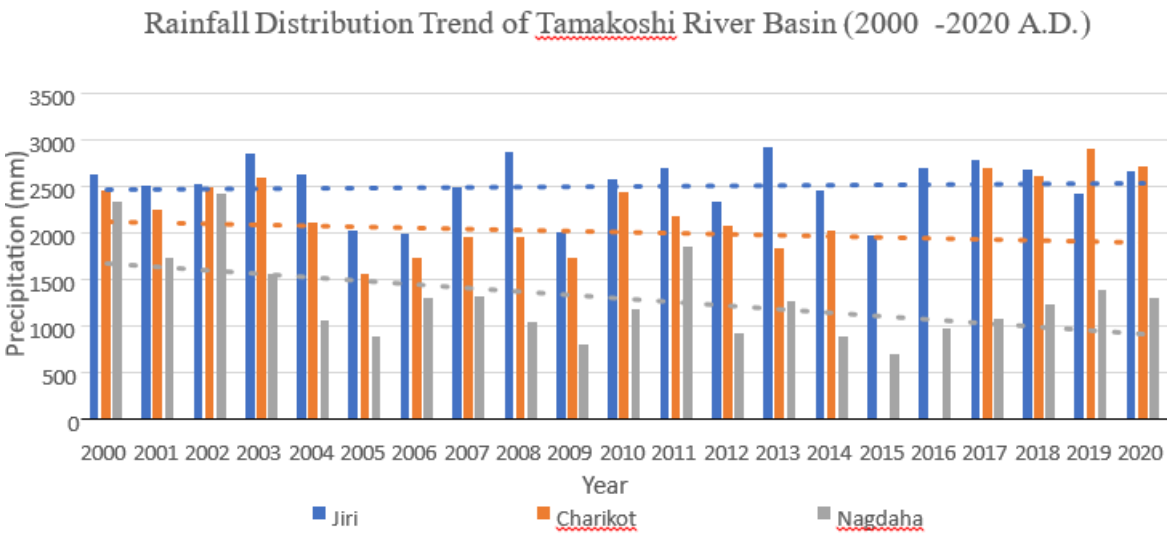

Figure 5: Rainfall distribution trend of Tamakoshi River Basin from 2000-2020.

Table 5: Annual peak flow data for Indrawati and Tamakoshi Rivers.

Year	Indrawati River (m^3/s)	Tamakoshi River (m^3/s)
2000	940	783
2001	957	811
2002	1053	770
2003	459	924
2004	827	862
2005	742	897
2006	1312	1270
2007	740	845
2008	810	940
2009	653	957
2010	851.7	1050
2011	774	459
2012	769.28	827
2013	758	742
2014	854	1270
2015	880	1310

3.3. Flood susceptible zone

The total sum of the weight of each contributing element analyzed is used to calculate the net risk of flooding in each flood susceptible zone. All contributing factor maps are overlaid to get this total aggregate weight. With the overlay process in GIS, the decision-maker can identify a list that meets a predefined set of criteria. The Raster Calculator in the ArcGIS Spatial Analyst tool is used for all of these procedures, including the compilation of contributing factor maps, the overlaying of all maps, and the estimation of susceptible regions. The factors which contribute to the floods are given in Table 7.

The ratios of factors according to their impacts on flood susceptibility are determined for Slope by 21.27%, Elevation by 26.6%, Land Use Land Cover by 26.6%, Rainfall Intensity by 15.95%, and Distance Away from River Network by 9.58%. The thematic maps shown in Fig. 5 are combined based on these proportions. The flood susceptible zone map is prepared by giving suitable ranks (10 is the highest; 2 is the lowest) to these contributing factors, and the prepared map is shown in Fig. 7. The area of the prepared map is divided into five classes: very low, low, moderate, high, and very high susceptible zones. In the case of the Indrawati River Basin, places like Palchok, Melamchi, Sindhukot, Sipapokhari, Bhimtar, Jyamire, and Duwachaur seem to be very high to high susceptible zones for flood events to occur. Similarly, in the case of the Tamakoshi River Basin, places like Nagdaha, Singati, Laduk, Bulung, and Lamidada are in very high to high susceptible zones for flood events to occur as shown in Fig. 8.

3.4. Flood return period

Flood frequency analysis is carried out for all the tributary inflows in the Indrawati River and Tamakoshi River based on 15-year annual peak flow data observed. Based on the methodology described above, the important parameters needed for the analysis are computed, and the various discharges expected alongside their return periods for the Indrawati River and Tamakoshi River are shown in Table 8. The maximum flood peak recorded in the Indrawati River was 1312 m^3/s in 2006, whereas Tamakoshi recorded its highest flood peak of 1310 m^3/s in 2006. The results from the table show that the expected stream discharge for return periods 2 years, 5 years, 10 years, 50 years, and 100 years are 809.55 m^3/s, 1012.23 m^3/s, 1146.42 m^3/s, 1441.75 m^3/s, 1566.59 m^3/s for Indrawati River. In contrast, the expected stream discharge for the same return periods is 973.10 m^3/s, 1200.34 m^3/s, 1350.78 m^3/s, 1681.89 m^3/s, 1821.87 m^3/s for Tamakoshi River. The expected discharge for the coming 100 years will be 1566.59 m^3/s for the Indrawati River and 1821.87 m^3/s for the Tamakoshi River. The results obtained shows an increasing trend in flood discharge for the return period of up to 100 years, as shown in Fig. 9.

Conclusion

The proposed study presents a practical approach to developing a flood susceptibility zone map of the Indrawati River Basin and Tamakoshi River Basin using GIS and RS techniques. The geodatabase developed from the study provides information on the flood susceptible of both river basins and can serve as a sound decision support system for flood hazard management. The research provides a detailed scenario of the flood susceptible zones, the current land use, and land classification patterns in the proposed study area. Multi-criteria evaluation methods have been applied in many studies and have successfully aided decision-making processes. Using the same evaluation method for our study, five different input maps were prepared: maps of slope, rainfall intensity,

Table 6: Overall weights and related susceptibility of flooding parameters.

A. Slope class (in degree)								
S.N.	Indrawati River Basin	Tamakoshi River Basin	Susceptibility Ranges	Proposed rate (a)	Rate (b)	Weighted Rate ($a * b$)	Total weight	Percentage (%)
1.	0-20	0-16	Very High	10		20		
2.	20-40	16-32	High	8		16		
3.	40-60	32-49	Moderate	6	2	12	60	21.27%
4.	60-80	49-65	Low	4		8		
5.	>80	65-82	Very Low	2		4		
B. Elevation Class (in meters above sea level)								
1.	572-1404	823-2035	Very High	10		25		
2.	1404-2192	2035-3247	High	8		20		
3.	2192-3133	3247-4459	Moderate	6	2.5	15	75	26.6%
4.	3133-4194	4459-5671	Low	4		10		
5.	4194-6147	5671-6883	Very Low	2		5		
C. LULC Class								
1	Water bodies, Ice/snow and Bareland	Water bodies, Ice/snow and Bareland	Very High	10	2.5	25	75	26.6%
2	Shrubland and Settlement	Shrubland and Settlement	High	8		20		
3	Vegetation Land	Grassland	Moderate	6		15		
4	Grassland	Vegetation Land	Low	4		10		
5	Forests	Forests	Very Low	2		5		
D. Rainfall Class (in millimeter)								
1.	908-1391	1285-1528	Very Low	2		3		
2.	1391-1873	1528-1770	Low	4		6		
3.	1873-2356	1770-2013	Moderate	6	1.5	9	45	15.95%
4.	2356-2839	2013-2255	High	8		12		
5.	2839-3321	2255-2498	Very High	10		15		
E. Distance Away from River Class (in meters)								
1.	0-500	0-500	Very High	10		15		
2.	500-1000	500-1000	Moderate	6	1.5	9	27	9.58%
3.	1000-1500	1000-1500	Low	2		3		

Table 7: Factors contributing to flood with their relative weight and percentage

S.N.	Flood causative factors	Unit	Hazard ratings	Total weights	Percentage (%)
1.	Slope	masl	10	60	21.27%
2.	Elevation	Degree	8	75	26.6%
3.	Land use	Meter	6	75	26.6%
4.	Rainfall	mm	4	45	15.95%
5.	Distance away from river network	Meter	2	27	9.58%

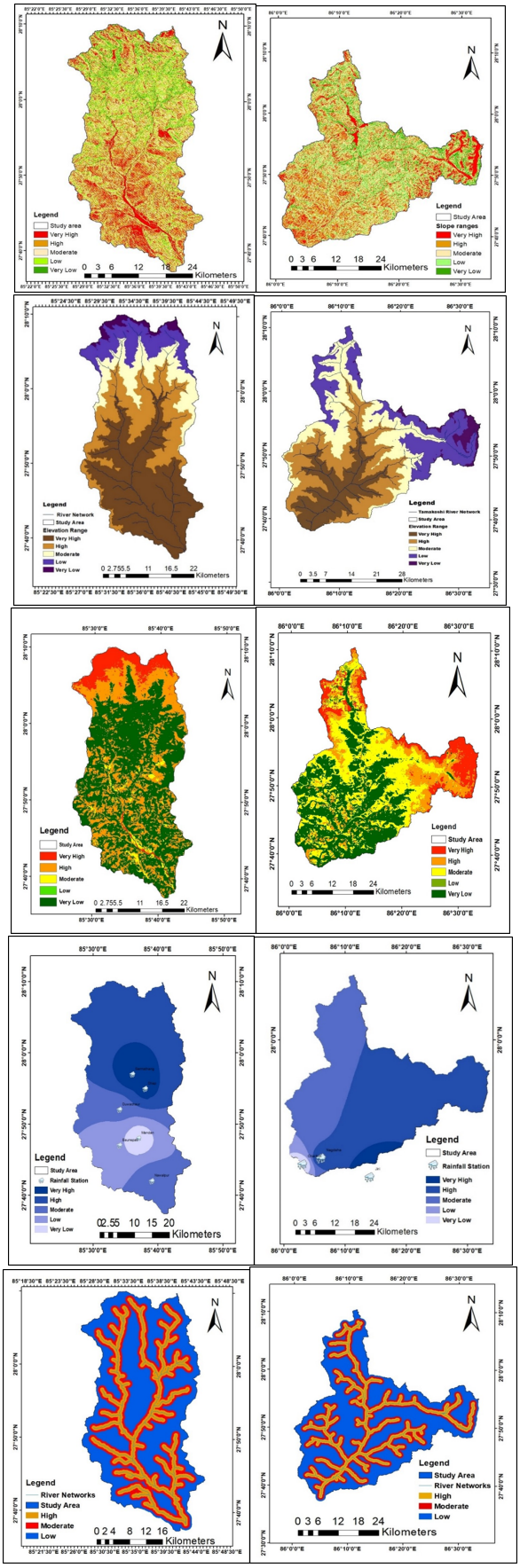

Figure 6: Thematic weightage map of flood factors of Indrawati River Basin (Left) and Tamakoshi River Basin (Right) a-b) Slope, c-d) elevation, e-f) LULC, g-h) Rainfall, i-j) Distance away from river network.

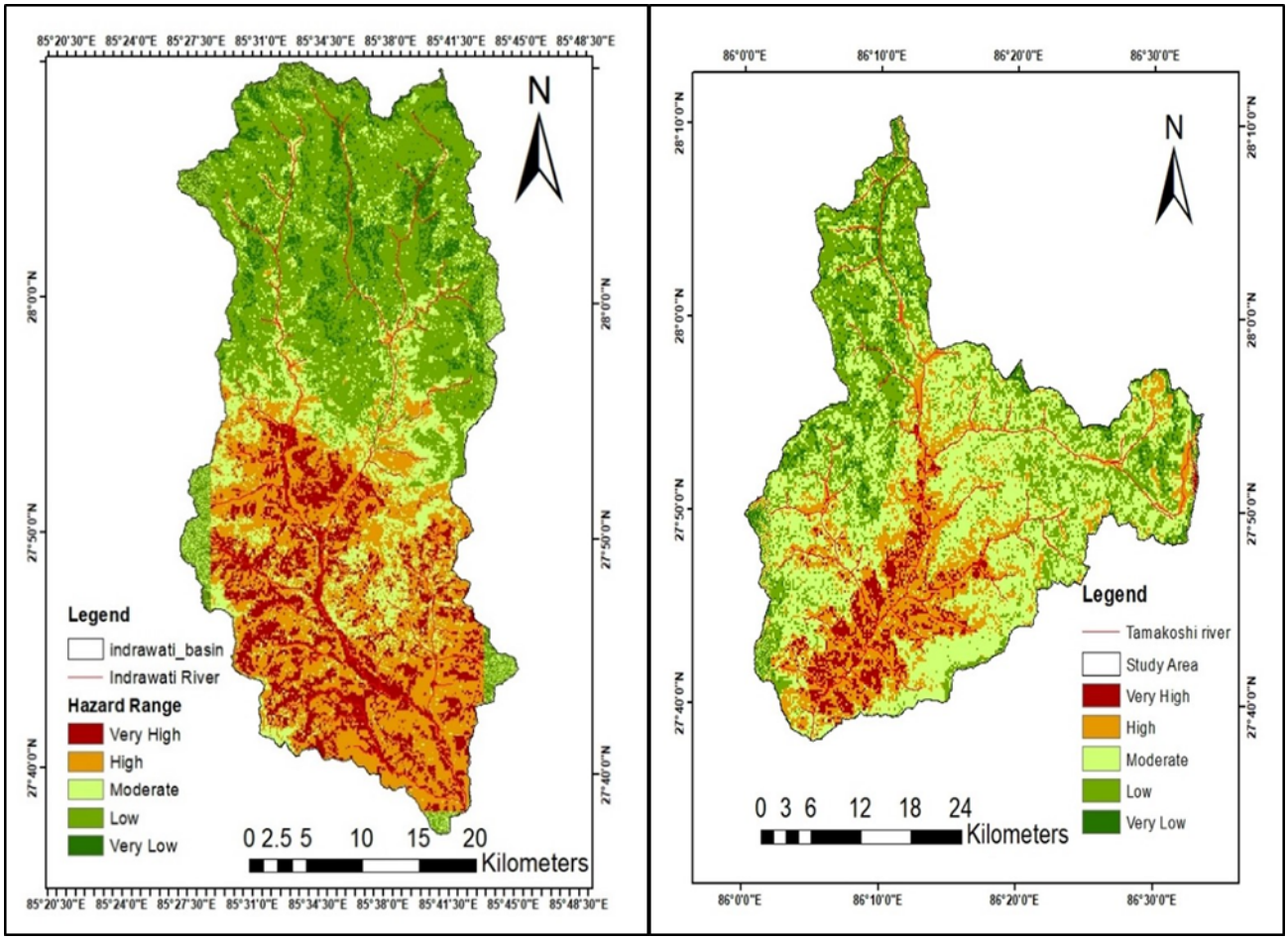

Figure 7: a) Flood susceptibility zone map of Indrawati River basin b) Flood susceptibility zone map of Tamakoshi River basin.

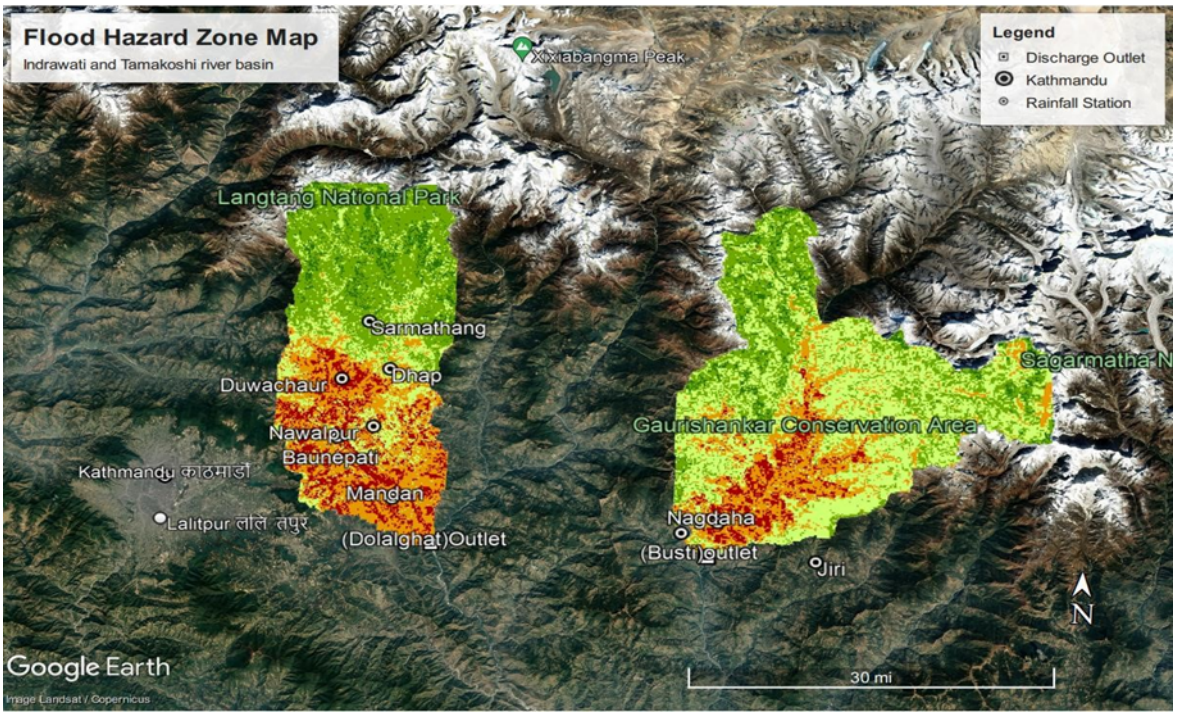

Figure 8: Flood susceptibility zone in Google Earth.

Table 8: Computation of expected flood along Indrawati River and Tamakoshi River.

Return Period (T)	River	Reduced Variate	Frequency Factor	Expected Flood (m^3/s)
2 Years	Indrawati	0.3665	-0.1446	809.55
2 Years	Tamakoshi	0.3665	-0.1446	973.10
5 Years	Indrawati	1.4999	0.9541	1012.23
5 Years	Tamakoshi	1.4999	0.9541	1200.34
10 Years	Indrawati	2.2504	1.6815	1146.42
10 Years	Tamakoshi	2.2504	1.6815	1350.78
50 Years	Indrawati	3.9019	3.2825	1441.75
50 Years	Tamakoshi	3.9019	3.2825	1681.89
100 Years	Indrawati	4.6001	3.9593	1566.59
100 Years	Tamakoshi	4.6001	3.9593	1821.87

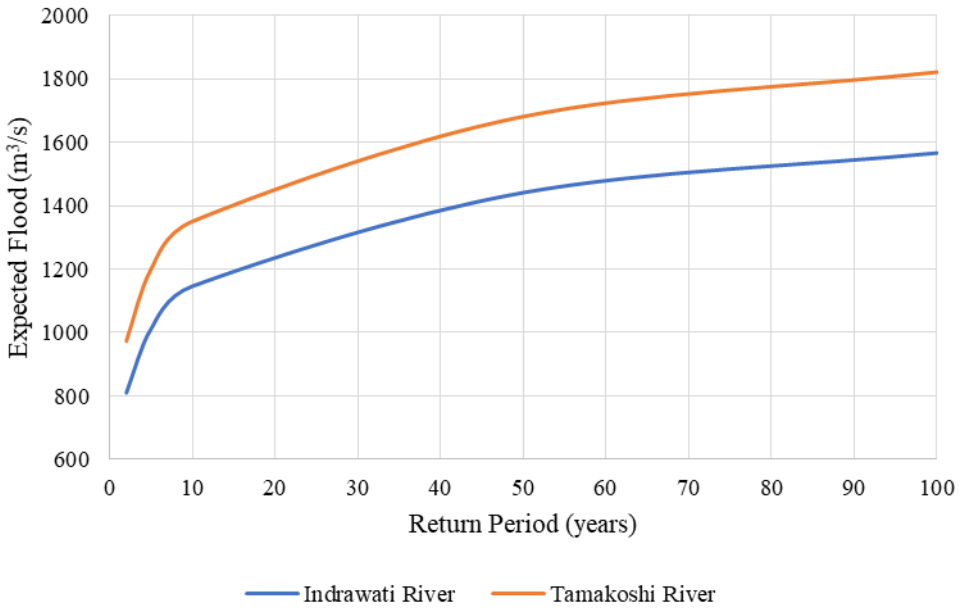

Figure 9: Plot of expected flood in different return periods for Indrawati River and Tamakoshi River.

elevation, land use, land cover, and distance away from the river network. The flood susceptible map of the Indrawati River Basin indicates that downstream plains of the basin part, Dalchok, Melamchi, Sindhukot, Sipapokhari, Bhimtar, Jyamire, and Duwachaur are within very high to high flood susceptible zones. Likewise, the Tamakoshi River Basin, mostly the downstream plain of basin parts Nagdaha, Singati, Laduk, Bulung, and Lamidada, are within very high to high flood susceptible zones. Therefore, it is possible to conclude that elements at risk, particularly people, towns, settlements, and vegetation in both basin areas, are subjected to high flood risk. Hence, those areas need immediate attention to alleviate potential flood risk. The estimation of flood discharge in various return periods using the statistical approach of Gumbel's method gives us the relation between expected flow (discharge) and return period, which will be beneficial in the engineering design of hydrological facilities such as stormwater drains, culverts, and reservoirs in order to safeguard people and property downstream of the river. From our study, a significant increase in flood discharge can be seen for the return period of 2 to 100 years. The expected discharge for the coming 100 years will be 1,566.59 m^3/s for the Indrawati River and 1,821.87 m^3/s for the Tamakoshi River. By knowing the estimated flood discharge for upcoming years, the hydrologic structures can be built resiliently. A limitation of this method of flood susceptibility mapping is that the GIS result is not combined with an applicable hydrologic/hydraulic method for estimating stages. As a result, the study concluded without any hydrodynamic simulation or estimation of flood depth inundation. Therefore, future research on developing flood susceptibility maps that can indicate the depth of inundation through hydrodynamic simulation should be done for the Indrawati River basin and Tamakoshi River basin. For future studies, a detailed field survey can be conducted to assess the study area and surrounding settlements better. Higher-resolution images can be utilized to improve the accuracy of the analysis. Additionally, incorporating factors such as flow accumulation, soil type, proximity to roads, and drainage density could enhance the development of the susceptibility zone map.

References

[1] Syvitski J P, Overeem I, Brakenridge G R & Hannon M, Floods, floodplains, delta plains - A satellite imaging approach, *Sedimentary Geology*, 267–268 (2012) 1–14. ISSN 0037-0738. https://doi.org/10.1016/j.sedgeo.2012.05.014.

[2] Dahal D, Ale Magar B, Aryal A, Poudel B, Banjara M & Kalra A, Analyzing climate dynamics and developing machine learning models for flood prediction in Sacramento, California, *Hydroecology and Engineering*, 1(1) (2024) 10003–10003. ISSN 3007-5319. https://doi.org/10.70322/hee.2024.10003.

[3] Tembata K & Takeuchi K, Floods and exports: An empirical study on natural disaster shocks in Southeast Asia, *Economics of Disasters and Climate Change*, 3(1) (2018) 39–60. ISSN 2511-1299. https://doi.org/10.1007/s41885-018-0033-6.

[4] Parajuli A, Parajuli R, Banjara M, Bhusal A, Dahal D & Kalra A, Application of machine learning and hydrological models for drought evaluation in ungauged basins using satellite-derived precipitation data, *Climate*, 12(11) (2024) 190. ISSN 2225-1154. https://doi.org/10.3390/cli12110190.

[5] Chan F K S, Wang Z, Chen J, Lu X, Nafea T, Montz B, Adekola O, Pezzoli A, Griffiths J, Peng Y, Li P & Wang J, Selected global flood preparation and response lessons: Implications for more resilient Chinese Cities, *Natural Hazards*, 118(3) (2023) 1767–1796. ISSN 1573-0840. https://doi.org/10.1007/s11069-023-06102-x.

[6] Dahal D, Shrestha S, Poudel B, Banjara M & Kalra A, The role of reclaimed water in urban flood management: Public perception and acceptance, *Earth Science Research*, 14(1) (2024) 1. ISSN 1927-0542. https://doi.org/10.5539/esr.v14n1p1.

[7] Nepal Climate Vulnerability Study Team (NCVST), Vulnerability through the eyes of vulnerable: Climate change induced uncertainties and Nepal's development predicaments, *Institute for Social and Environmental Transition (ISET)*.

[8] Neupane N. *To Study the Various Factors Affecting the Summer Monsoon Rainfall in Nepal*. Master's thesis, The University of Texas at Austin, Jackson School of Geoscience, Department of Atmospheric Science (2008).

[9] Dixit A, Floods and vulnerability: Need to rethink flood management, *Natural Hazards*, 28(1) (2003) 155–179. ISSN 0921-030X. https://doi.org/10.1023/a:1021134218121.

[10] United Nations International Strategy for Disaster Reduction (UNISDR). *2009 Global Assessment Report on Disaster Risk Reduction: Risk and Poverty in a Changing Climate*. United Nations.

[11] Government of Nepal, Ministry of Home Affairs and DP-Net-Nepal. Nepal disaster report 2015: Avalanche from Gangapurna Himal in Manang (2015).

[12] Bajracharya S R, Pradhananga S, Shrestha A B & Thapa R, Future climate and its potential impact on the spatial and temporal hydrological regime in the Koshi Basin, Nepal, *Journal of Hydrology: Regional Studies*, 45 (2023) 101316. ISSN 2214-5818. https://doi.org/10.1016/j.ejrh.2023.101316.

[13] Ghimire M & Timalsina N, Assessment of denudation rate and erosion susceptibility in the upper Tamakoshi basin in the higher Himalayas, Nepal, *Geographical Journal of Nepal*, 14 (2021) 41–80. ISSN 0259-0948. https://doi.org/https://doi.org/10.3126/gjn.v14i0.35548.

[14] Water and Energy Commission Secretariat (WECS). *Water Resource of Nepal in the Context of Climate Change*. Government of Nepal, Water and Energy Commission Secretariat (2011).

[15] Liu W, Carling P A, Hu K, Wang H, Zhou Z, Zhou L, Liu D, Lai Z & Zhang X, Outburst floods in China: A review, *Earth-Science Reviews*, 197 (2019) 102895. ISSN 0012-8252. https://doi.org/10.1016/j.earscirev.2019.102895.

[16] Maharjan S B, Steiner J F, Shrestha A B, Maharjan A et al. The Melamchi flood disaster: Cascading hazard and the need for multihazard risk management. Tech. rep. (2021). URL https://www.icimod.org/article/the-melamchi-flood-disaster/.

[17] Gautam M, Evaluation and comparison of curve numbers based on dynamic land use and land cover changes, *Current Trends in Civil & Structural Engineering*, 11(3). ISSN 2643-6876. https://doi.org/10.33552/ctcse.2024.11.000764.

[18] Kalra A, Shrestha S, Dahal D, Banjara M, Paudel B & Gupta R. Assessing the performance of hec-hms and swmm models for rainfall–runoff simulation for urban watershed. In: *World Environmental and Water Resources Congress 2025*. American Society of Civil Engineers (2025), pp. 1230–1242. https://doi.org/10.1061/9780784486184.112.

[19] Ale Magar B, Acharya K, Babu Ghimire A & Shin S. Evaluating the resilience of hybrid centralized and decentralized water supply systems. In: *World Environmental and Water Resources Congress 2024*. American Society of Civil Engineers (2024), pp. 1316–1325. https://doi.org/10.1061/9780784485477.118.

[20] da Silva L B L, Alencar M H & de Almeida A T, Multidimensional flood risk management under climate changes: Bibliometric analysis, trends and strategic guidelines for decision-making in urban dynamics, *International Journal of Disaster Risk Reduction*, 50 (2020) 101865. ISSN 2212-4209. https://doi.org/10.1016/j.ijdrr.2020.101865.

[21] Chaulagain D, Ram Rimal P, Ngando S N, Nsafon B E K, Suh D & Huh J S, Flood susceptibility mapping of Kathmandu Metropolitan City using GIS-based multi-criteria decision analysis, *Ecological Indicators*, 154 (2023) 110653. ISSN 1470-160X. https://doi.org/10.1016/j.ecolind.2023.110653.

[22] Douglas I, Climate change, flooding and food security in South Asia, *Food Security*, 1(2) (2009) 127–136. ISSN 1876-4525. https://doi.org/10.1007/s12571-009-0015-1.

[23] Momblanch A, Holman I & Jain S, Current practice and recommendations for modelling global change impacts on water resource in the Himalayas, *Water*, 11(6) (2019) 1303. ISSN 2073-4441. https://doi.org/10.3390/w11061303.

[24] Adhikari T R, Baniya B, Tang Q, Talchabhadel R, Gouli M R, Budhathoki B R & Awasthi R P, Evaluation of post-extreme floods in a high mountain region: A case study of the melamchi flood 2021 at the koshi river basin in nepal, *Natural Hazards Research*, 3(3) (2023) 437–446. ISSN 2666-5921. https://doi.org/10.1016/j.nhres.2023.07.001.

[25] Wiegant D, Living on the edge in the Nepalese Indrawati river basin; A study on water-induced stress and hazards and the factors that determine the resilience of himalaya communities. https://doi.org/10.13140/RG.2.2.30094.15680.

[26] Chen Y, Flood hazard zone mapping incorporating geographic information system (GIS) and multi-criteria analysis (MCA) techniques, *Journal of Hydrology*, 612 (2022) 128268. ISSN 0022-1694. https://doi.org/10.1016/j.jhydrol.2022.128268.

[27] Samanta S, Pal D K & Palsamanta B, Flood susceptibility analysis through remote sensing, gis and frequency ratio model, *Applied Water Science*, 8(2). ISSN 2190-5495. https://doi.org/10.1007/s13201-018-0710-1.

[28] Choudhary R & Pathak D, Land use/land cover change detection through temporal imageries and its implications in water induced disaster in Triyuga watershed, East Nepal, *Journal of Nepal Geological Society*, 51 (2016) 49–54. ISSN 0259-1316. https://doi.org/10.3126/jngs.v51i0.24087.

[29] Verburg P H, van de Steeg J, Veldkamp A & Willemen L, From land cover change to land function dynamics: A major challenge to improve land characterization, *Journal of Environmental Management*, 90(3) (2009) 1327–1335. ISSN 0301-4797. https://doi.org/10.1016/j.jenvman.2008.08.005.

[30] Wang Y, Fang Z, Hong H, Costache R & Tang X, Flood susceptibility mapping by integrating frequency ratio and index of entropy with multilayer perceptron and classification and regression tree, *Journal of Environmental Management*, 289 (2021) 112449. ISSN 0301-4797. https://doi.org/10.1016/j.jenvman.2021.112449.

[31] Megahed H A, Abdo A M, AbdelRahman M A E, Scopa A & Hegazy M N, Frequency ratio model as tools for flood susceptibility mapping in urbanized areas: A case study from Egypt, *Applied Sciences*, 13(16) (2023) 9445. ISSN 2076-3417. https://doi.org/10.3390/app13169445.

[32] Asadollahi A, Magar B A, Poudel B, Sohrabifar A & Kalra A, Application of machine learning models for improving discharge prediction in ungauged watershed: A case study in East DuPage, Illinois, *Geographies*, 4(2) (2024) 363–377. ISSN 2673-7086. https://doi.org/10.3390/geographies4020021.

[33] Soliman M, Morsy M M & Radwan H G, Assessment of implementing land use/land cover LULC 2020-ESRI global maps in 2D flood modeling application, *Water*, 14(23) (2022) 3963. ISSN 2073-4441. https://doi.org/10.3390/w14233963.

[34] Akram AlSukker M E Marah Al-Saleem, Flood risk map using a multi-criteria evaluation and geographic information system: Wadi Al-Mafraq Zone., *Jordan Journal of Mechanical & Industrial Engineering*, 16(2) (2022) 291–300. ISSN 1995-6665.

[35] Rahman R & Saha S K, Remote sensing, spatial multi criteria evaluation (SMCE) and analytical hierarchy process (AHP) in optimal cropping pattern planning for a flood prone area, *Journal of Spatial Science*, 53(2) (2008) 161–177. ISSN 1836-5655. https://doi.org/10.1080/14498596.2008.9635156.

[36] Fell R, Corominas J, Bonnard C, Cascini L, Leroi E & Savage W Z, Guidelines for landslide susceptibility, hazard and risk zoning for land use planning, *Engineering Geology*, 102(3–4) (2008) 85–98. ISSN 0013-7952. https://doi.org/10.1016/j.enggeo.2008.03.022.

[37] Gómez-Gutiérrez A, Conoscenti C, Angileri S E, Rotigliano E & Schnabel S, Using topographical attributes to evaluate gully erosion proneness (susceptibility) in two mediterranean basins: advantages and limitations, *Natural Hazards*, 79(S1) (2015) 291–314. ISSN 1573-0840. https://doi.org/10.1007/s11069-015-1703-0.

[38] Hagos Y G, Andualem T G, Yibeltal M & Mengie M A, Flood hazard assessment and mapping using GIS integrated with multi-criteria decision analysis in upper Awash River basin, Ethiopia, *Applied Water Science*, 12(7). ISSN 2190-5495. https://doi.org/10.1007/s13201-022-01674-8.

[39] Ozkan S P & Tarhan C, Detection of flood hazard in urban areas using GIS: Izmir case, *Procedia Technology*, 22 (2016) 373–381. ISSN 2212-0173. https://doi.org/10.1016/j.protcy.2016.01.026.

[40] Shrestha S, Dahal D, Poudel B, Banjara M & Kalra A, Flood susceptibility analysis with integrated geographic information system and analytical hierarchy process: A multi-criteria framework for risk assessment and mitigation, *Water*, 17(7) (2025) 937. ISSN 2073-4441. https://doi.org/10.3390/w17070937.